High-precision calculation of relativistic corrections for hydrogen-like atoms with screened Coulomb potentials

Hui Xie[1], Li Guang Jiao[1], Ai Liu[1], and Y.K. Ho[2]

[1]Jilin University
[2]Institute of Atomic and Molecular Sciences Academia Sinica

January 27, 2021

Abstract

The first-order relativistic corrections to the non-relativistic energies of hydrogen-like atom embedded in plasma screening environments are calculated in the framework of direct perturbation theory by using the generalized pseudospectral method. The standard Debye-Hückel potential, exponential cosine screened Coulomb potential, and Hulthén potential are employed to model different screening conditions and their effects on the eigenenergies of hydrogen-like atoms are investigated. The relativistic corrections which include the relativistic mass correction, Darwin term, and the spin-orbit coupling term for both the ground and excited states are reported as functions of screening parameters. Comparison with previous theoretical predictions shows that both the relativistic mass correction and spin-orbit coupling obtained in this work are in good agreement with previous estimations, while significant discrepancy and even opposite trend is found for the Darwin term. The overall relativistic-corrected system energies predicted in this work, however, are in good agreement with the fully relativistic calculations available in the literature. We finally present the scaling law of the first-order relativistic corrections and discuss the validity of the direct perturbation theory with respect to both the nuclear charge and the screening parameter.

E-mail address: lgjiao@jlu.edu.cn

Introduction

Investigation of the plasma screening effect on the embedded atoms has been of considerable interest in the interdisciplinary areas of atomic and molecular physics, plasma physics, condensed matter physics, and astrophysics (Margenau & Lewis, 1959; Ichimaru, 1982; Murillo et al., 2013; Stanton & Murillo, 2015). In the past few decades, several models have been proposed and widely used to simulate the structure variation, response, and reaction dynamics of atomic systems in different types of plasmas. The most representative and also simplest screening model is the Debye-Hückel or Yukawa model (Debye & Hückel, 1923; Ugalde et al., 1997; Sil et al., 2009; Janev et al., 2016; Zan et al., 2017; Zhu et al., 2020), where the charged particles are interacted through an exponential screened Coulomb potential (SCP). Such a model has been extensively used to simulate the collective electronic screening effects of weakly-coupled classical plasmas on the charged particle interactions. Its significance in describing the shielding effects of charged mobile carriers on the impurity ion in the semiconductor or quantum dot has also been revealed (Kwon, 2006; Genkin & Lindroth, 2010). On the other hand, the strongly-coupled dense quantum plasmas can be effectively modeled by an exponential cosine screened Coulomb potential (ECSCP) or cosine-Debye-Hückel potential (Shukla & Eliasson, 2008; Shukla & Eliasson, 2010; Shukla & Eliasson, 2012). It has also been well-known for a long time that the ECSCP has wide applications in modeling the screening environment in solid-state physics (McIrvine, 1960; Hall, 1962; Krieger, 1969). Another important and simplified short-range potential applied to model the screening effect in plasmas and other environments is the Hulthén potential (HP)

(Hulthén, 1942; Varshni, 1990; Bahar et al., 2016). It shows similar behavior as the SCP in short range but is systematically weaker than both the SCP and ECSCP. It can also be employed to perturbatively approximate the SCP in weak screening conditions (Lam & Varshni, 1971) due to the fact that charged particles interacting with HP in s-wave symmetry are analytically solvable.

In the past few years, there has been a wealth of theoretical studies on the abundant physical properties of atoms interacting with the three types of model potential. The variation of system energies has been thoroughly investigated by many numerical methods such as the variational method (Roussel & O'Connell, 1974; Greene & Aldrich, 1976; Stubbins, 1993), $1/N$ expansion method (Roy, 1986; Chatterjee, 1987; Sever & Tezcan, 1987), the asymptotic iteration method (Ciftci et al., 2003; Bayrak & Boztosun, 2007), the perturbation method (McEnnan et al., 1976; Lai, 1982), the generalized pseudospectral method (Roy, 2005; Roy, 2013; Roy, 2016), etc. Other interesting properties of the screened atom include the state radiative transition and lifetime (Qi et al., 2008; Qi et al., 2016), static and dynamic polarizabilities (Qi et al., 2009; Das, 2012; Kar et al., 2018), multiphoton excitation and ionization (Qi et al., 2009; Qi et al., 2017), classical and quantum information-theoretic investigations (Isonguyo et al., 2018; Abdelmonem et al., 2017), resonances (Bylicki et al., 2007; Nasser et al., 2011), and electron-atom scattering processes (Qi et al., 2013; Karmakar & Ghoshal, 2019). Reviewing these works one may find that most of the researches were performed in the framework of non-relativistic theory, i.e. the solution of Schrödinger equation. Some fully relativistic calculations on specific physical properties are also available in the literature (see, for example, Refs. (Filippin et al., 2014; Krauthauser & Hill, 2002)) which, by necessity, rely on the accurate solution of the relativistic Dirac equation. On the other hand, for light atoms or ions with relatively small nuclear charge, the relativistic effects can be efficiently and also accurately taken into account by using the direct perturbation theory. For the one-electron system eigenenergies investigated in this work, these effects reduce to the well-known three terms including the relativistic mass correction, the Darwin term, and the spin-orbit coupling term (Bethe & Salpeter, 2008; Zhu et al., 2020).

The systematic investigation on the relativistic effects in hydrogen-like ions embedded in Debye plasmas modeled by SCP has been performed by Bielińska-Wąż et al. (Bielińska-Wąż et al., 2004). The authors presented the analytical first-order perturbative corrections to the system energies for several lower-lying bound states and verified that the first-order perturbation theory gives a very good approximation to the locations of energy levels for ionized atoms in plasmas. The variation of fine-structure splittings and the relativistic effects on excitation transition rates were also examined for different ions in various screening conditions. The subsequent work of Poszwa (Poszwa, 2012), based on the expansion of wave function into Sturmian functions, focused on the accurate computation of relativistic corrections for the screened hydrogen-like atoms in SCP and HP models. Non-relativistic and the overall (three-term summed) first-order relativistic corrections for bound states with $n \leq 4$ and $j = l - 1/2$ were reported with high accuracy. The effectiveness of the direct perturbation theory is then confirmed by the same author (Poszwa & Bahar, 2015) for hydrogen-like ions with nuclear charge up to 40, through a comparison with the fully relativistic calculations of the Dirac equation. The most recent work of Chaudhuri et al. (Chaudhuri et al., 2017) solved the non-relativistic energies and the first-order relativistic corrections by expanding the system wave function in terms of Slater-type orbitals which, to the best of our knowledge, is the first investigation on the individual contribution of the three relativistic terms on atomic structure under screening confinements. The variations of relativistic mass correction, Darwin term, and spin-orbit splitting for the ground as well as the first two p-wave excited states of hydrogen-like ions (from C^{5+} to Ti^{21+}) embedded in both SCP and ECSCP are provided for a wide range of screening parameters. After careful examining the numerical values reported by the authors, however, we find that there exist quite large discrepancies between the authors' calculations and the predictions by Poszwa (Poszwa, 2012), especially at large screening parameters. The aims of our present work are therefore three folds: (1) we would like to provide, in the framework of first-order direct perturbation theory, a systematic investigation on the three relativistic correction terms for screened hydrogen-like ions with SCP, ECSCP, and HP models, in both the ground and excited states, (2) resolve the discrepancies between previous predictions by providing fully converged, highly accurate calculations based on a different theoretical method, and (3) discuss the applicability of the direct perturbation theory with

2

respect to both the nuclear charge and the screening parameter.

This paper is organized as follows. In Sec. II, we briefly outline the theoretical method in accurately solving the Schrödinger equation and formulate the first-order relativistic corrections in different screened Coulomb potentials, followed by the derivation of scaling laws with respect to the nuclear charge. In Sec. III, we present comprehensive comparison of our numerical calculations with previous predictions and some general discussions about the validity of the direct perturbation treatment of relativistic effects. Sec. IV is devoted to the summary and conclusion. Atomic units are used throughout the paper ($\hbar = m_e = e = 1$) and the speed of light $c = 137.035999084$ is adopted according to the recommendation of CODATA2018 (Mohr et al., 2016).

Theoretical method

Generalized pseudospectral method

In this section, we present an overview of the GPS method for accurately solving the Schrödinger equation of hydrogen-like ions in the non-relativistic framework. Only essential steps will be introduced and more details can be found in Refs. (Roy, 2005; Roy, 2013; Roy, 2016; Zhu et al., 2020; Yao & Chu, 1993; Chu & Telnov, 2004) and references therein. The radial Schrödinger equation for one-electron system can be written as

$$\left[-\frac{1}{2}\frac{d^2}{dr^2} + \frac{l(l+1)}{2r^2} + V(r) \right] \psi_{nl}(r) = E_{nl}\psi_{nl}(r),$$

(1)

where

$$V(r) =$$

$$\begin{cases} -\frac{Ze^{-\lambda r}}{r}, & \text{for SCP,} \\ -\frac{Ze^{-\lambda r}}{r}\cos(\lambda r), & \text{for ECSCP,} \\ -\frac{Z\lambda e^{-\lambda r}}{1-e^{-\lambda r}}, & \text{for HP,} \end{cases}$$

(2)

in which λ denotes the characteristic screening parameter, n and l refer to, respectively, the principle and orbital angular quantum numbers, and Z the atomic nuclear charge. All three types of screened Coulomb potential reduce to the Coulomb potential at the limit of $\lambda = 0$. Except for the special case of Hulthén potential in s-wave symmetry (with eigenenergy $E_{n0} = -(2Z - \lambda n^2)^2/(8n^2)$ (Varshni, 1990)), there are no analytical solutions for Eq. 1 with potential in Eq. 2 and some numerical approximations must be made.

The GPS method solves the differential equation in the scheme of discretized variable representation. The semi-infinite domain $r \in [0, \infty]$ is firstly mapped onto a finite one $x \in [-1, 1]$ through the following non-linear mapping function

$$r \equiv f(x) = L\frac{1+x}{1-x},$$

(3)

where L is an adjustable mapping parameter. The radial wave function is then transformed by $\phi(x) = \sqrt{f'(x)}\psi(f(x))$ and substituted into Eq. 1. The transformed radial Schrödinger equation now reads

$$\left[-\frac{1}{2f'(x)}\frac{d^2}{dx^2}\frac{1}{f'(x)} + \frac{l(l+1)}{2f(x)^2} + V(f(x)) \right]\phi(x) = E\phi(x).$$

(4)

The key step in performing the GPS method is to approximate the smooth, unknown function $\phi(x)$ by a N-th order polynomial $\phi_N(x)$ (Yao & Chu, 1993; Chu & Telnov, 2004), i.e.

$$\phi(x) \approx \phi_N(x) = \sum_{j=0}^{N} \phi(x_j)g_j(x),$$

(5)

where x_j are the collocation points with $x_0 = -1$, $x_N = 1$, and $x_{j,(j=1,\dots,N-1)}$ are roots of the first derivative of Legendre polynomial $L_N(x)$, and $g_j(x)$ are cardinal functions fulfilling the delta-like relation $g_j(x_i) = \delta_{ij}$.

The Dirichlet boundary condition $\psi(0) = \psi(\infty) = 0$ for physical bound states leads to $\phi(-1) = \phi(1) = 0$, which further simplifies the $(N+1)$-dimensional eigenvalue problem into a $(N-1)$-dimensional one. After performing a symmetric procedure, Eq. 4 is finally converted into a standard and symmetric eigenvalue problem

$$\sum_{j=1}^{N-1} H_{ij}A_j = EA_i,$$

(6)

where

$$A_j = \frac{\sqrt{f'(x_j)}\psi(f(x_j))}{L_N(x_j)},$$

(7)

and

$$H_{ij} = -\frac{1}{2}\frac{1}{f'(x_i)}(d_2)_{ij}\frac{1}{f'(x_j)} + \frac{l(l+1)}{2f(x_i)^2}\delta_{ij} + V(f(x_i))\delta_{ij},$$

4

(8)

with the second-order differential matrix given by (Canuto et al., 2006)

$$(d_2)_{ij} =$$

$$
\begin{cases}
-\frac{N(N+1)}{3(1-x_i^2)}, & i = j \in [1, N-1], \\
-\frac{2}{(x_i-x_j)^2}, & i \neq j, i, j \in [1, N-1].
\end{cases}
$$
(9)

Relativistic corrections

According to the direct perturbation theory (Bethe & Salpeter, 2008), the first-order relativistic correction to the non-relativistic energy of one-electron system is give by

$$E^{(1)} = \frac{1}{4c^2}\left(-2\langle(V - E^{(0)})^2\rangle + \frac{1}{2}\langle\nabla^2 V\rangle + \left\langle\boldsymbol{\sigma}\cdot\boldsymbol{L}\frac{1}{r}\frac{dV}{dr}\right\rangle\right).$$

(10)

Here we use the notation $\langle O \rangle \equiv \langle\Psi|O|\Psi\rangle$ as the expectation value of an operator O with respect to the non-relativistic (zero-order) wave function Ψ. Therefore, the zero-order energy $E^{(0)}$ is exactly the eigenenergy of the Schrödinger equation solved by Eq. 1. The three terms on the right-hand side of the above formula is known as the relativistic mass correction (or the relativistic correction to kinetic energy) E_m, the Darwin term E_D, and the spin-orbit coupling term E_{so}, respectively. The more concrete form of these terms are given by (Poszwa, 2012; Chaudhuri et al., 2017)

$$E_m = -\frac{1}{2c^2}(E^{(0)})^2 + \frac{1}{c^2}E^{(0)}\langle V\rangle - \frac{1}{2c^2}\langle V^2\rangle,$$

(11)

$$E_D = \frac{1}{8c^2}\langle\nabla^2 V\rangle =$$

$$
\begin{cases}
-\frac{\lambda^2 Z}{8c^2}\left\langle\frac{e^{-\lambda r}}{r}\right\rangle + \frac{Z}{8c^2}\langle\frac{\delta(r)}{r^2}\rangle, & \text{for SCP,} \\
-\frac{\lambda^2 Z}{4c^2}\left\langle\frac{e^{-\lambda r}\sin(\lambda r)}{r}\right\rangle + \frac{Z}{8c^2}\langle\frac{\delta(r)}{r^2}\rangle, & \text{for ECSCP,} \\
\frac{\lambda^2 Z}{8c^2}\left\langle\frac{e^{-\lambda r}}{(1-e^{-\lambda r})^2}\left(\frac{2}{r} - \frac{\lambda(1+e^{-\lambda r})}{1-e^{-\lambda r}}\right)\right\rangle + \frac{Z}{8c^2}\langle\frac{\delta(r)}{r^2}\rangle, & \text{for HP,}
\end{cases}
$$
(12)

5

and

$$E_{so} = \frac{1}{4c^2} \left(j(j+1) - l(l+1) - \frac{3}{4} \right) \left\langle \frac{1}{r} \frac{\mathrm{d}V}{\mathrm{d}r} \right\rangle,$$

(13)

where $j = \left| l \pm \frac{1}{2} \right|$ is the quantum number of the spin-orbit coupled angular momentum and

$$\frac{\mathrm{d}V}{\mathrm{d}r} =$$

$$\begin{cases} \frac{\lambda r + 1}{r^2} Z e^{-\lambda r}, & \text{for SCP,} \\ \frac{(\lambda r + 1)\cos(\lambda r) + \lambda r \sin(\lambda r)}{r^2} Z e^{-\lambda r}, & \text{for ECSCP,} \\ \frac{\lambda^2}{(1 - e^{-\lambda r})^2} Z e^{-\lambda r}, & \text{for HP.} \end{cases}$$

(14)

The calculation of expectation values in the framework of GPS is quite straightforward. Taking the radial expectation value in m-th power ($m \geq -2l - 1$) as an example, the integration is conveniently transformed into a finite summation

$$\langle r^m \rangle = \int_{-1}^{1} |\phi(x)|^2 f(x)^m dx = \sum_{j=1}^{N-1} A_j^2 f(x_j)^m,$$

(15)

where A_j are available directly from the eigenvectors of eigenvalue problem shown in Eq. 6. However, due to the Dirichlet boundary condition for bound states has been explicitly incorporated into the GPS method, one cannot obtain the value of radial wave function at the origin. Such a fact causes significant effect in the calculations of quantities such as $\langle r^{-2(l+1)} \rangle$ and $\langle \delta(\boldsymbol{r}) \rangle$. In Ref. (Zhu et al., 2020), we have successfully introduced an extrapolation technique (Press et al., 1992) to extract the information of wave function at the origin and applied it to calculate various expectation values of physical quantities for confined atoms. The numerical accuracy are generally in the same level as those obtained directly from the GPS method. Such a technique is used in the present work to calculate the relativistic mass correction and Darwin term on account of, respectively, the contributions from $\langle V^2 \rangle$ and $\langle \delta(\boldsymbol{r}) \rangle$. The spin-orbit coupling term is only applicable for non-s states and, therefore, there is no need to supplement the contributions from the origin.

6

Z-scaling law

Recalling the fact that one can always introduce the Z-scaling transformations of radial variable and screening parameter (Poszwa, 2012)

$$\rho = Zr, \ \mu = \frac{\lambda}{Z},$$

(16)

into the Schrödinger equation, so as to express the non-relativistic system energy in a Z-independent form

$$\varepsilon^{(0)}(\mu) = \frac{E^{(0)}(Z, \lambda)}{Z^2},$$

(17)

the scaling law for the first-order relativistic corrections shown in Eqs. 10–13 can correspondingly be derived as

$$\varepsilon^{(1)}(\mu) = \frac{E^{(1)}(Z, \lambda)}{Z^4}.$$

(18)

The relativistic-corrected energy for a hydrogen-like ion with nuclear charge Z is immediately obtained by

$$E_{rel}(Z, \lambda) = Z^2 \varepsilon^{(0)}(\mu) + Z^4 \varepsilon^{(1)}(\mu).$$

(19)

In what follows, we will focus on the system with $Z = 1$, i.e. the hydrogen atom, rewriting μ and $\varepsilon^{(0,1)}$ by λ and $E^{(0,1)}$ for convenience.

The Z-scaling laws shown in Eqs. 17 and 18 can be utilized to test the accuracy of numerical calculations. This is done in our following discussion about the accuracy of the GPS method employed in this work. From Eq. 19 we can easily find that the contribution of the first-order relativistic effect increases two times faster than the non-relativistic energies when the atomic number Z is increased. Therefore, the direct perturbation theory should not be applicable for highly charged ions. Another aspect that we would like to emphasis and discuss later is that, for a screening parameter being close to the critical value λ_c where the bound state acquires zero non-relativistic energy and then merges into the continuum (Varshni, 1990; Roy, 2016; Varshni, 2001; Diazt et al., 1991), the corresponding relativistic corrections might not be zero. In such a situation, the direct perturbation theory does not work as well.

Results and discussion

Non-relativistic energies

Table 1: Scaling law of the non-relativistic energy and the first-order relativistic correction for the ground state of hydrogen-like ions with SCP. The calculations on systems with extremely high Z are included just for illustrative purposes.

μ	Z	λ	$E^{(0)}$	$E^{(1)}c^2$
0.1	1	0.1	-0.40705803061340315675450707036	-0.12275428491853096631564955919 2
0.1	10	1	-0.40705803061340315675450707036 1(+2)	-0.1227542849185309663156495591 91(+4)
0.1	100	10	-0.40705803061340315675450707036 1(+4)	-0.1227542849185309663156495591 90(+8)
1.0	1	1	-0.1028578999001769680477421531 44(-1)	-0.1992268748709012854872299827 05(-1)
1.0	10	10	-0.1028578999001769680477421531 43(+1)	-0.1992268748709012854872299827 05(+3)
1.0	100	100	-0.1028578999001769680477421531 44(+3)	-0.1992268748709012854872299827 06(+7)

Figure 1: Variation of the non-relativistic energies for some lower-lying bound states ($n \leq 5$, $l \leq 3$) of H atom in various screening environment as functions of screening parameter. In each group of states in the same n shell, the orbital angular momentum l increases from right to left. (a) SCP, (b) ECSCP, and (c) HP.

The robustness of GPS method in solving the radial Schrödinger equation has been well-established and here we show some examples on the accuracy of numerical calculations. In Table 1, the non-relativistic energy

and the first-order relativistic correction for the ground state of one-electron systems are shown for scaled screening parameter $\mu = 0.1$ and 1.0. A total number of $N = 600$ points are used, the mapping parameter is adjusted by setting $L = \langle r \rangle$, and all calculations are performed in quadruple precision (~ 34 significant digits). It is found that both $E^{(0)}$ and $E^{(1)}c^2$ follow very well the Z-scaling laws defined in Eqs. 17 and 18 (~ 30 significant digits). The increasing of N would slightly increase the convergence because the utilization of $N = 600$ is large enough for us to have access to the quadruple-precision arithmetic limit. The calculations are somewhat less sensitive with respect to L. The highly accurate results shown in Table 1 also demonstrate that the extrapolation technique introduced in Sec. II. C is quite effective.

The non-relativistic spectra of hydrogen atom in the three types of screened Coulomb potential, i.e. SCP, ECSCP, and HP, are illustrated in Fig. 1 (a), (b), and (c), respectively. Numerical results at some selected values of λ are provided in the Supplementary Material. The variation of spectrum in the screening environment has been extensively discussed by many authors, we present some general trends as follows: (1) the screened Coulomb potentials with non-zero values of screening parameter only support finite number of bound states due to their short-range character, (2) the l degeneracy of bound states in the same n shell is destroyed and the spectrum is systematically lifted up when the screening strength is enhanced, and (3) with continuously increasing the screening parameter to specific critical values, the bound states would eventually acquire zero eigenenergies and then merge into the continuum. It is worth mentioning here that very accurate critical screening parameters for a variety of bound states of hydrogen atom in SCP, ECSCP, and HP are available in the literature (Varshni, 1990; Roy, 2016; Varshni, 2001; Diazt et al., 1991). The present GPS calculations implemented in quadruple precision can successfully reproduce the benchmark values with more than 9 digits.

Relativistic corrections

Figure 2:   Relativistic mass correction for some lower-lying bound states ($n \leq 5$, $l \leq 3$) of H atom in various screening environment as functions of screening parameter. In each group of states with same l symmetry, the principle quantum number n increases from top to bottom. (a) SCP, (b) ECSCP, and (c) HP.

figures/fig4a/fig4a-eps-converted-to.pdf
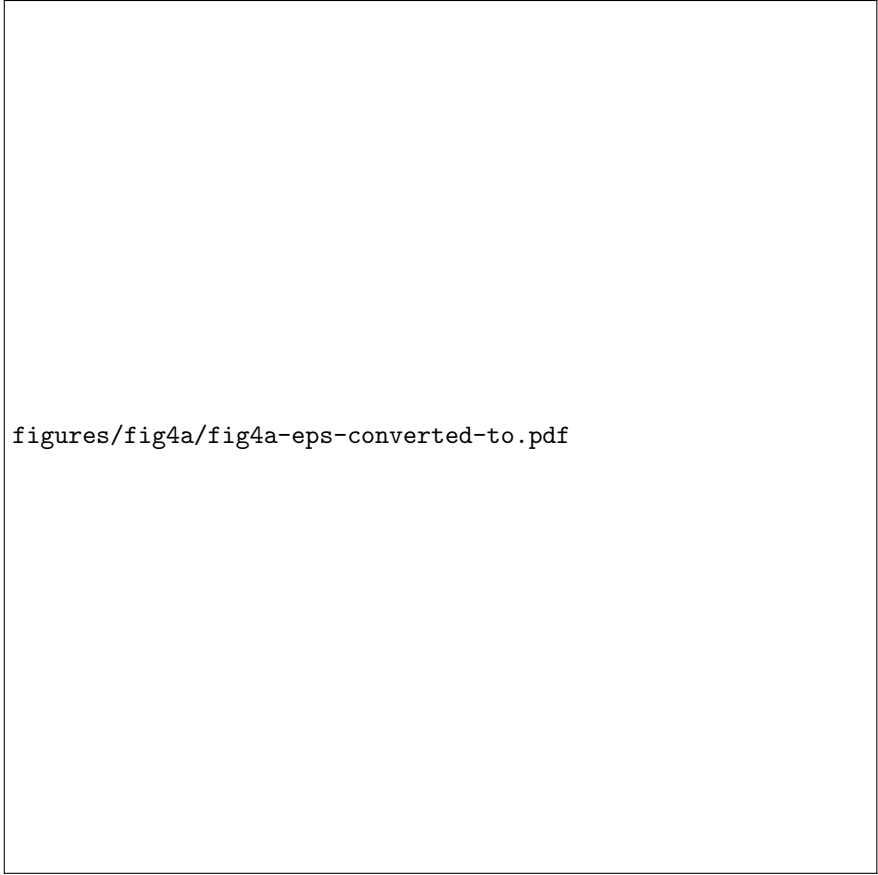
Figure 3: Same as Fig. 2 but for the Darwin term. They are positive and negative for s- and non-s-wave states, respectively. (a, d) SCP, (b, e) ECSCP, and (c, f) HP.
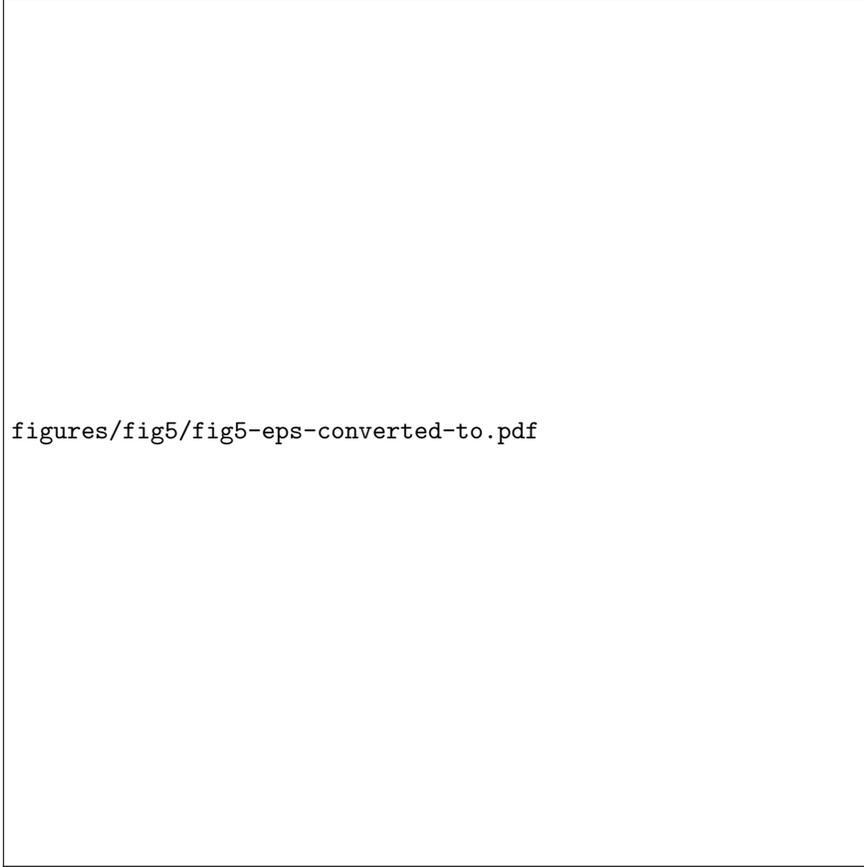
Figure 4: Same as Fig. 2 but for the spin-orbit splitting which is defined by $\Delta E_{so} = E_{so,\ j=l+1/2} - E_{so,\ j=l-1/2}$ for non-s-wave states only. (a) SCP, (b) ECSCP, and (c) HP.

The relativistic corrections for one-electron system include the relativistic mass correction E_m, the Darwin term E_D, and the spin-orbit coupling term E_{so}. From Eqs. 10–13 we know that the relativistic mass correction exists in all bound states, while the spin-orbit coupling only shows up in non-s-wave states. The Darwin term comes from two components, one from the screened character of interaction potential and the other from the amplitude of wave function at the origin. Therefore, it is expected that the Darwin terms are non-zero for all s-wave states, while for non-s-wave states they only exist in the screened situation where $\lambda \neq 0$. Considering the Z-scaling laws shown in Eqs. 17–19, we explicitly show in the Supplementary Material a complete list of the non-relativistic energy $E^{(0)}$ and the overall first-order relativistic correction $E^{(1)}c^2$ for the bound states ($n \leq 4$, $l \leq 3$) of H atom embedded in SCP, ECSCP, and HP. For SCP and HP, the calculations of Poszwa (Poszwa, 2012) by using an expansion method based on Sturmain functions are included for comparison. For ECSCP, there are no predictions available in the literature and we compare with the fully relativistic calculations of Poszwa and Bahar (Poszwa & Bahar, 2015) by solving the Dirac equation. Input parameters of $N = 400$ and $L = \langle r \rangle$ are used in the present GPS calculations and the reported numerical values are fully converged in all digits shown in the tables. It is found that our results are in excellent agreement with the previous predictions when they are available and, furthermore, the agreement in ECSCP demonstrates that the first-order direct perturbation approximation is well applied for low-Z hydrogen-like ions (Poszwa, 2012; Poszwa & Bahar, 2015).

The individual variation of relativistic mass correction, the Darwin term, and spin-orbit coupling as functions of screening parameter are illustrated in Figs. 2, 3, and 4, respectively, for H atom in the three screening

12

potentials. The calculations for each bound state are performed for screening parameters starting from zero up to corresponding critical value. It is clear that the relativistic mass correction takes negative values whose magnitude decreases continuously when the potential screening strength is increased. The same trend is followed by the spin-orbit splitting term except that they are positive. The Darwin term, as discussed above, shows significant discrepancies between s- and non-s-wave states. From Fig. 3 (a–c), it is shown that the Darwin term for s-wave states decreases monotonically from its unscreened value. Such a trend is expected from Eq. 12 on account of the fact that, as increasing λ the wave function become more diffused in the radial distribution and, as a result, its amplitude at the origin decreases. The other component which stems from the screened character of potential takes a negative value, and its contribution is generally enlarged. The Darwin term for non-s-wave states shown in Fig. 3 (d–f) solely comes from the first component and they are always negative. For relatively small values of λ where the radial density distribution of wave function does not change much under the influence of screened potential, the Darwin term follows approximately a quadratic law with respect to λ, i.e. $E_D \propto -C\lambda^2$, as we can simply derive from Eq. 12. With continuously increasing λ the expectation-value term decreases drastically because of the delocalization of radial wave function. The competition of these two effects leads to a maximum of Darwin term located at screening parameter close to the corresponding critical value.

From Figs. 2–4, it is interestingly found that, at critical screening parameters λ_c where the "bound" states have zero non-relativistic energies, the three relativistic corrections are actually non-zero in spite of their extremely small quantities. This is understood as follows. The Dirichlet boundary conditions $\psi(0) = \psi(\infty) = 0$ holds only for bound states with $E^{(0)} < 0$. When $\lambda = \lambda_c$ and $E^{(0)} = 0$ where the bound state transforms into a quasi-bound or continuum state, the boundary conditions in such cases are known to be $\psi(0) = 0$ and $\psi(\infty) = \text{constant} = 1$ (normalized condition) (Diazt et al., 1991; Varshni & Kesarwani, 1978). Therefore, all three terms are non-zero and the overall relativistic corrections to eigenenergies are correspondingly non-zero (with very small magnitude). We further comment that the above discussion are ideal cases on the assumption of the applicability of direct perturbation theory. For practical purposes, the fully relativistic calculations based on Dirac equation would shed more light on such critical phenomena.
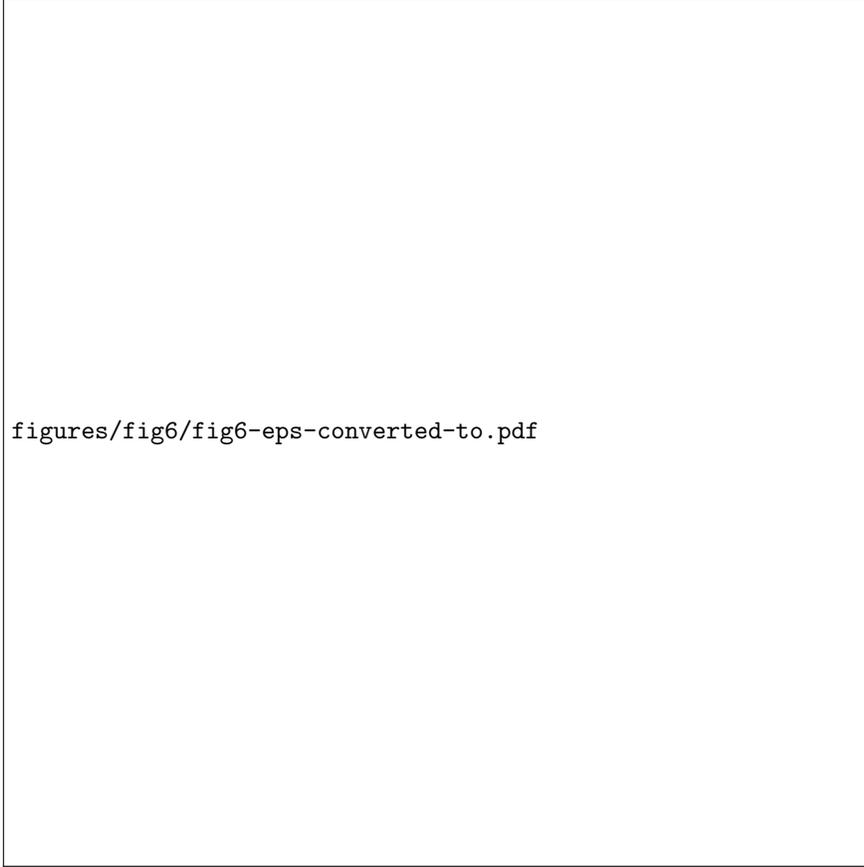
Figure 5: Comparison of the non-relativistic energy $E^{(0)}$, the relativistic mass correction E_m, and the Darwin term E_D for the ground state energies of C^{5+} ion in SCP, ECSCP, and HP. Lines are present calculations and dots are from Chaudhuri et al. (Chaudhuri et al., 2017). (a) $E^{(0)}$, (b) E_m, and (c) E_D.

In the following discussion, we would like to take a detailed comparison with the predictions of Chaudhuri et al. (Chaudhuri et al., 2017) who employed the basis-set expansion method based on Slater-type orbitals. The authors presented systematic investigations on individual relativistic correction terms for hydrogen-like ions with $Z = 6$–22, in both SCP and ECSCP. Keeping in mind that the Z-scaling law is applicable for the iso-electronic sequence, we only show in Table 2 the comparison of E_m and E_D for the ground state of C^{5+} in SCP. Also included in the table are the calculations of relativistic-corrected energy $E = E^{(0)} + E^{(1)}$ by Poszwa (Poszwa, 2012) using a similar method but on Sturmian functions. The comparisons of $E^{(0)}$, E_m, and E_D for all three types of screened Coulomb potential are demonstrated in Fig. 5 for an overview. It is interestingly found that although our calculations on $E^{(0)}$ and E_m are in good agreement with the predictions of Chaudhuri et al. (Chaudhuri et al., 2017), the Darwin term E_D, however, show opposite changes as varying the screening parameter. Similar situation is found on the Darwin term for all the ground states of H iso-electronic sequence with both SCP and ECSCP.

It is noted from Table 2 and comparison in the Supplementary Material that the present results show excellent agreement with the calculations of Poszwa (Poszwa, 2012). For further comparison, we list in Table 3 the present and Chaudhuri et al. (Chaudhuri et al., 2017)'s first-order relativistic corrections and the fully relativistic calculation of Poszwa and Bahar (Poszwa & Bahar, 2015) for the ground state of Ca^{19+} in ECSCP. The present relativistic-corrected energies are in better agreement with the fully relativistic results of Poszwa and Bahar (Poszwa & Bahar, 2015) in all cases. The divergence with respect to the Darwin term

14

accounts for the main part of discrepancies in the total system energy. It is also noted that the relativistic mass corrections show larger discrepancies at relatively large screening parameters. We keep in mind that both the present and Chaudhuri et al. (Chaudhuri et al., 2017)'s calculations successfully reproduce the analytical result of Darwin term at $\lambda = 0$ where the wave function at the origin contributes solely. Hence, it is reasonably conjectured that the divergence would come from the estimation of expectation-value contribution with respect to the screened Coulomb potentials.

Table 4 presents the comparison of non-relativistic energy $E^{(0)}$ and separate relativistic correction terms, i.e. E_m, E_D, and E_{so}, for the $2p$ excited state of C^{5+} in both SCP and ECSCP. Good agreement is found between the present estimations and those in Chaudhuri et al. (Chaudhuri et al., 2017), except for the cases when the screening parameters are close to $\lambda_c(2p)$. We also notice that at $\lambda = 1.4$ and 0.9 for SCP and ECSCP, respectively, the authors predicted a positive energy for $2p$ state as well as finite values for the three relativistic terms. Such calculations are not feasible in the present GPS method due to they are not bound states.

Relativistic effect on charged ions

Figure 6: Ratios of the first-order relativistic correction $E^{(1)}$ to the non-relativistic energy $E^{(0)}$ as functions of λ_c-scaled screening parameter for the ground state of hydrogen-like ions with $Z = 1$–40 in SCP. The gray area represents the parameter space where the direct perturbation theory is not applicable.

15
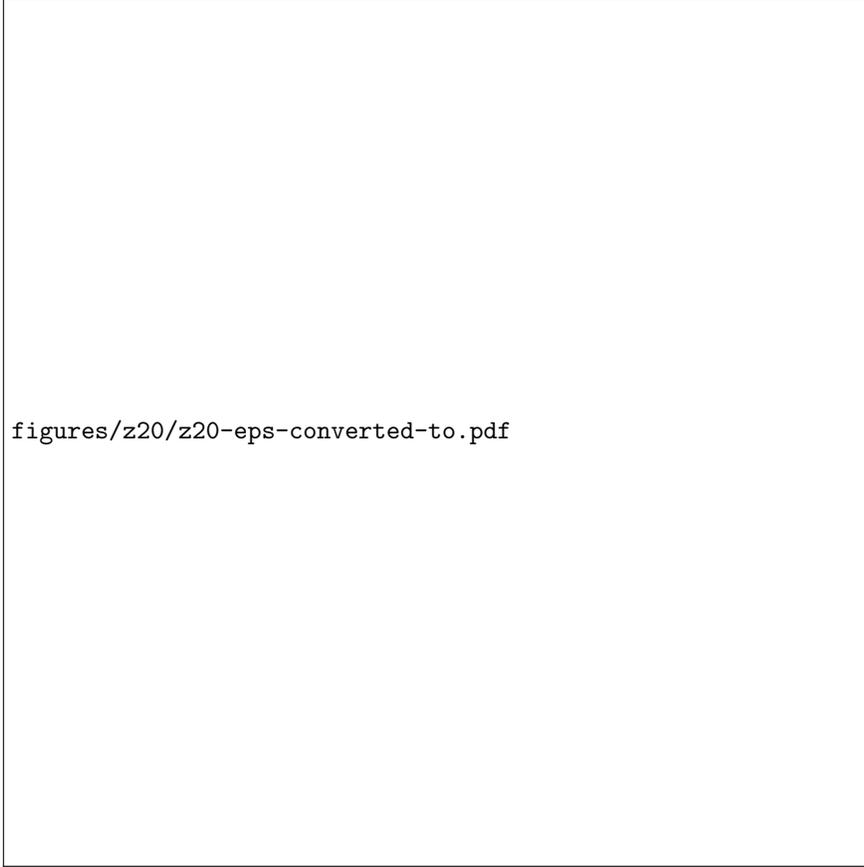
Figure 7: Non-relativistic energy and the first-order relativistic correction for the ground state of Ca^{19+} as functions of screening parameter in SCP, ECSCP, and HP. $E^{(0)}$ and $E^{(1)}$ refer to left and right ordinates, respectively.

In Table 3 we have shown that the non-relativistic energy combined with the first-order relativistic correction approximates very well to the fully relativistic energy of hydrogen-like ion with $Z = 20$ in a wide range of screening parameters. On the other hand, the scaling law shown in Eq. 19 reveals a fact that the relativistic correction increases much faster than the non-relativistic energy as increasing Z. Therefore, it would be of great interest to investigate the applicability of the direct perturbation theory in the combined parameter space of λ and Z. Fig. 6 displays the ratio of the first-order relativistic correction to the non-relativistic energy defined by $\sigma = E^{(1)}/E^{(0)}$ as functions of re-scaled screening parameter λ/λ_c for some selected nuclear charge Z. For all ions investigated here, the modification of system energy by relativistic effects is smallest in the pure Coulomb situation. It is found that σ would increase monotonically for increasing the screening strength, and eventually approach to infinity at λ_c due to $E^{(0)} = 0$ but $E^{(1)} \neq 0$. Taking $\sigma < 0.1$ as the tentative criteria for the validity of the direct perturbation theory, it is generally concluded that the first-order relativistic correction applies very well for low- and intermediate-Z ions, with the range of screening parameter λ diminishing slightly for increasing Z.

We finally show in Fig. 7 a comparison of the non-relativistic energy and the relativistic corrections in different screened Coulomb potentials for the ground state of Ca^{19+}. The critical screening parameters are 40.0, 23.812, and 14.410 for HP, SCP, and ECSCP, respectively. For a one-electron system, in virtue of the relation $V_{CP} \leq V_{HP} \leq V_{SCP} \leq V_{ECSCP}$ and the comparison theory (Stubbins, 1993; Wang, 1992) for Schrödinger equation, we can immediately obtain the inequality of energy as $E_{CP}^{(0)} \leq E_{HP}^{(0)} \leq E_{SCP}^{(0)} \leq$

16

$E^{(0)}_{ECSCP}$. However, as one can see from Fig. 7, the first-order relativistic correction does not have such a relationship, especially between $E^{(1)}_{SCP}$ and $E^{(1)}_{ECSCP}$. The same behavior can also be found in Fig. 5 for the ground state of C^{5+}, where both the relativistic mass correction and Darwin term cross each other at a specified screening parameter. Nevertheless, the relativistic-corrected energies $E = E^{(0)} + E^{(1)}$ (not shown in Fig. 7 because they are indistinguishable from the curves of $E^{(0)}$) still follow the prediction of comparison theory due to the fact that $E^{(1)}$ are several orders of magnitude smaller than $E^{(0)}$.

Conclusion

In this work, we have applied the GPS method to solve the radial Schrödinger equation for various bound states of hydrogen-like ions in SCP, ECSCP, and HP. The obtained highly accurate non-relativistic energies and wave functions are then employed to calculate the first-order relativistic corrections in the framework of direct perturbation theory. It has been shown that the magnitude of relativistic mass correction and spin-orbit coupling for all bound states and the Darwin term for s-wave states decreases monotonically if the screening effect is enhanced continuously. The Darwin term for non-s-wave states, however, increases rapidly from zero, reaching to the maximum at a relatively large screening parameter, and then decreases to a finite value at the corresponding critical screening parameter. Our numerical results are thoroughly compared with previous basis-set expansion predictions. Excellent agreement is found between the present results with those available in the literature obtained by utilizing Sturmian functions, while quite large discrepancies exist in the comparison with the one using Slater-type orbitals. The possible reason for such a disagreement is discussed. The applicability of the direct perturbation theory with respect to the screening parameter and nuclear charge is analyzed in detail. We generally conclude that the perturbation theory can be reasonably applied to low- and intermediate-Z hydrogen-like ions, with the effective range of screening parameters diminishing for increasing Z. In the vicinity of critical screening parameters where the bound states tend to merge into the continuum, as well as for the systems of highly-charged ions immersed in screening environments, the perturbation theory fails and one needs to explicitly deal with the fully relativistic Dirac equation. Such researches will be investigated in our future work.

Acknowledgements

Conflict of Interest

We declare that we do not have any commercial or associative interest that represents a conflict of interest in connection with the work submitted here.

Supporting Information

The Supplementary Material attached to the present manuscript provides a complete list and detailed comparison of the non-relativistic and relativistic-corrected energies for a variety of bound states of H atom in SCP, ECSCP, and HP.

(missing citation)

17

Table 2: Comparison of the non-relativistic energy $E^{(0)}$, the relativistic mass correction E_m, the Darwin term E_D, and the relativistic-corrected energy $E = E^{(0)} + E^{(1)}$ for the ground state of hydrogen-like C^{5+} with SCP. "a" and "b" refer to the calculations by Chaudhuri et al. (Chaudhuri et al., 2017) and Poszwa (Poszwa, 2012), respectively. Numbers in parentheses represent the power of ten.

λ	$E^{(0)}$	E_m	E_D	$E = E^{(0)} + E^{(1)}$
0.0	-0.18000000000000000000(+2)	-0.43133597161550642224(-1)	0.34506877729240513779(-1)	-0.180086267194323...
a	-0.180000(+2)	-0.4313(-1)	0.3451(-1)	-0.1800862(+2)
0.1	-0.17407418517859090871(+2)	-0.43112444917501392016(-1)	0.34490427288445192949(-1)	-0.174160405354881...
a	-0.174074(+2)	-0.4311(-1)	0.3452(-1)	-0.1741599(+2)
0.2	-0.16829362081766378936(+2)	-0.43050561624145300164(-1)	0.34442303677742497180(-1)	-0.168379703397127...
a	-0.168294(+2)	-0.4305(-1)	0.3455(-1)	-0.1683790(+2)
0.4	-0.15715101482992056018(+2)	-0.42813164327018026177(-1)	0.34257706769099032732(-1)	-0.157236569405499...
a	-0.157151(+2)	-0.4282(-1)	0.3468(-1)	-0.1572324(+2)
0.5	-0.15178117029475488390(+2)	-0.42641471270731927347(-1)	0.34124203338026577242(-1)	-0.151866342974081...
a	-0.151781(+2)	-0.4265(-1)	0.3477(-1)	-0.1518598(+2)
0.6	-0.14654089102082513643(+2)	-0.42436745027905181196(-1)	0.33965010827056979440(-1)	-0.146625608362833...
a	-0.146540(+2)	-0.4245(-1)	0.3488(-1)	-0.1466157(+2)
b	-0.1465408910207(+2)			-0.1466256083618(+2)
0.8	-0.13643620698402448000(+2)	-0.41934353818183206077(-1)	0.33574323307114359136(-1)	-0.136519807289135...
a	-0.136435(+2)	-0.4195(-1)	0.3514(-1)	-0.1365031(+2)
1.0	-0.12681326565304625861(+2)	-0.41317343122697589289(-1)	0.33094404292349440904(-1)	-0.126895495041349...
a	-0.126810(+2)	-0.4134(-1)	0.3548(-1)	-0.1268686(+2)
1.2	-0.11765106409290961856(+2)	-0.40595764499564403897(-1)	0.32532980720480535149(-1)	-0.117731691930700...
a	-0.117645(+2)	-0.4062(-1)	0.3587(-1)	-0.1176925(+2)
b	-0.1176510640928(+2)			-0.1177316919298(+2)
1.4	-0.10893080955511220025(+2)	-0.39778645256743239076(-1)	0.31896965355137331897(-1)	-0.109009626354128...
a	-0.108921(+2)	-0.3979(-1)	0.3632(-1)	-0.1089557(+2)
2.4	-0.71415390010266077979(+1)	-0.34525461981316201479(-1)	0.27799789441365590867(-1)	-0.714826467356655...
a	-0.7141539001032(+1)			-0.7148264673506(+1)
3.6	-0.38208926702093109480(+1)	-0.26455253257739239858(-1)	0.21467308855074859869(-1)	-0.382588061461197...
b	-0.3820892670216(+1)			-0.3825880614569(+1)
4.8	-0.16093549619049478752(+1)	-0.17433144967559004267(-1)	0.14306597985346782278(-1)	-0.161248150888716...
b	-0.1609354961906(+1)			-0.1612481508858(+1)
5.4	-0.87531097779007397595	-0.12824215760358025646(-1)	0.10600711044238809214(-1)	-0.877534482506193...
b	-0.875310977790			-0.877534482484
6.0	-0.37028843964063708497	-0.82672198448711382312(-2)	0.68922803625613602059(-2)	-0.371663379122946...
b	-0.370288439640			-0.371663379108

Table 3: Same as Table 2 but for the ground state of hydrogen-like Ca^{19+} with ECSCP. "a" and "b" refer to the calculations by Chaudhuri et al. (Chaudhuri et al., 2017) and Poszwa and Bahar (Poszwa & Bahar, 2015), respectively, where the latter ones are obtained by solving the fully relativistic Dirac equation. Numbers in parentheses represent the power of ten.

λ	$E^{(0)}$	E_m	E_D	$E = E^{(0)} + $
0.0	-0.2000000000000000000(+3)	-0.53251354520432891634(+1)	0.42601083616346313307(+1)	-0.201065027090408
a	-0.200000(+3)	-0.53251(+1)	0.42601(+1)	-0.2010650(+3)
0.2	-0.19600039503136935897(+3)	-0.53251131189026585046(+1)	0.42600909158327130301(+1)	-0.197065417234439
b	-0.1960003950(+3)			-0.1970761076(+3)
0.4	-0.19200312104371877076(+3)	-0.53249598328355965886(+1)	0.42599711899914902937(+1)	-0.193068109686562
b	-0.1920031208(+3)			-0.1930788004(+3)
0.5	-0.19000605792932006636(+3)	-0.53247953775786249438(+1)	0.42598427530875260666(+1)	-0.191071010553811
a	-0.190006(+3)	-0.53247(+1)	0.42621(+1)	-0.1910686(+3)
b	-0.1900060580(+3)			-0.1910817008(+3)
1.0	-0.18004698656827506722(+3)	-0.53225283888140899257(+1)	0.42580727261140756551(+1)	-0.181111442230975
a	-0.180047(+3)	-0.53219(+1)	0.42753(+1)	-0.1810936(+3)
b	-0.1800469864(+3)			-0.1811221316(+3)
1.3	-0.17410135310514757452(+3)	-0.53195504065903856260(+1)	0.42557481684604100911(+1)	-0.175165155343277
a	-0.174101(+3)	-0.53183(+1)	0.42924(+1)	-0.1751269(+3)
1.4	-0.17212582171205500669(+3)	-0.53182177570785344407(+1)	0.42547080630489434021(+1)	-0.173189331406084
a	-0.172126(+3)	-0.53167(+1)	0.43000(+1)	-0.1731427(+3)
1.5	-0.17015382277680726707(+3)	-0.53166972601173756517(+1)	0.42535214265594278971(+1)	-0.171216998610365
a	-0.170154(+3)	-0.53149(+1)	0.43087(+1)	-0.1711602(+3)
2.0	-0.16035390985579127672(+3)	-0.53059333726936709971(+1)	0.42451227343786806374(+1)	-0.161414720494106
a	-0.160354(+3)	-0.53019(+1)	0.43701(+1)	-0.1612858(+3)
b	-0.1603539096(+3)			-0.1614253936(+3)
2.5	-0.15067144207573046925(+3)	-0.52890860543166390618(+1)	0.42319811817388894001(+1)	-0.151728546948308
a	-0.150671(+3)	-0.52818(+1)	0.44660(+1)	-0.1514868(+3)
2.9	-0.14302459108217906024(+3)	-0.52705662224665402346(+1)	0.42175382740719889228(+1)	-0.144077619030573
a	-0.143024(+3)	-0.52598(+1)	0.45718(+1)	-0.1437120(+3)
3.0	-0.14112797618986065528(+3)	-0.52651774542539057041(+1)	0.42133362381038127074(+1)	-0.142179817406010
a	-0.141128(+3)	-0.52534(+1)	0.46027(+1)	-0.1417787(+3)

Table 4: Comparison of the non-relativistic energy $E^{(0)}$, the relativistic mass correction E_m, the Darwin term E_D, and the spin-orbit splitting E_{so} for the $2p$ state of hydrogen-like C^{5+} with SCP and ECSCP. At each λ, the upper and lower values refer to the present calculations and Chaudhuri et al. (Chaudhuri et al., 2017), respectively. Numbers in parentheses represent the power of ten.

λ	$E^{(0)}$	E_m	E_D	E_{so}
0.0	-0.45000000000000000000(+1)	-0.12580632505452270649(-2)	-0.00000000000000000000	0.2156679858077532…
	-0.45000(+1)	-0.1258(-2)	-0.0000	0.2157(-2)
0.1	-0.39242267001422700080(+1)	-0.12478898413572424103(-2)	-0.55918705306759162530(-6)	0.2141397981252562…
	-0.39242(+1)	-0.1248(−2)	-0.5592(−6)	0.2141(−2)
0.2	-0.33942172396060618738(+1)	-0.12195100307229144321(-2)	-0.20781441014818062612(-5)	0.2098623412987159…
	-0.33943(+1)	-0.1220(−2)	-0.2078(−5)	0.2099(−2)
0.4	-0.24589405220019876749(+1)	-0.11185170520181424280(-2)	-0.70631924555678937946(-5)	0.1944933233287153…
	-0.24590(+1)	-0.1119(−2)	-0.7063(−5)	0.1945(−2)
0.5	-0.20490146715875436710(+1)	-0.10500847643452042140(-2)	-0.10077949239901002996(-4)	0.1839514134572007…
	-0.20490(+1)	-0.1050(−2)	-0.1008(−4)	0.1839(−2)
0.6	-0.16752380575220859019(+1)	-0.97203547572531580993(-3)	-0.13149539475119555527(-4)	0.1717973166723616…
	-0.16752(+1)	-0.9720(−3)	-0.1315(−4)	0.1718(−2)
0.8	-0.10313731553375941372(+1)	-0.79289305787062678061(-3)	-0.18610193283461030680(-4)	0.1433250095640687…
	-0.10314(+1)	-0.7929(−3)	-0.1861(−4)	0.1433(−2)
1.0	-0.52140885352455732283	-0.59052812949063395702(-3)	-0.21695607348129916682(-4)	0.1100150138791166…
	-0.5214	-0.5905(−3)	-0.2170(−4)	0.1100(−2)
1.2	-0.14765927510822725398	-0.36646087402336680263(-3)	-0.20103782163487558959(-4)	0.7118357688527353…
	-0.1645	-0.3849(−3)	-0.2088(−4)	0.7515(−3)
1.3	-0.19680162034544718227(-1)	-0.22833705379400729870(-3)	-0.15313499392818844637(-4)	0.4566302078996673…
	-0.193(-1)	-0.2325(−3)	-0.1560(−4)	0.4642(−3)
1.4	(unbound)			
	0.1302	-0.1055(-3)	-0.8097(-5)	0.2195(-3)
0.1	-0.39015727784159449991(+1)	-0.12568517722808661373(-2)	-0.73439462363078043700(-7)	0.2154886607288435…
	-0.39016(+1)	-0.1257(-2)	-0.7344(-7)	0.2155(-2)
0.2	-0.33118997825494852702(+1)	-0.12490978719965065086(-2)	-0.53928072146042060141(-6)	0.2143396735089830…
	-0.33119(+1)	-0.1249(-2)	-0.5393(-6)	0.2143(-2)
0.3	-0.27381244479023177048(+1)	-0.12299276429699153419(-2)	-0.16664881845511531356(-5)	0.2114913663796591…
	-0.27381(+1)	-0.1230(-2)	-0.1666(-5)	0.2115(-2)
0.4	-0.21861782834415849767(+1)	-0.11956538394992060253(-2)	-0.36027172442188614905(-5)	0.2063737276806471…
	-0.21862(+1)	-0.1196(-2)	-0.3603(-5)	0.2064(-2)
0.5	-0.16613519901275354255(+1)	-0.11431549086017646826(-2)	-0.63786731190958691494(-5)	0.1984729488423509…
	-0.16614(+1)	-0.1143(-2)	-0.6379(-5)	0.1985(-2)
0.6	-0.11688769865085986738(+1)	-0.10692019631213785634(-2)	-0.98966999531319766759(-5)	0.1872130843498484…
	-0.11688(+1)	-0.1069(-2)	-0.9897(-5)	0.1872(-2)
0.7	-0.71472293543211057030	-0.96922107054971645195(-3)	-0.13885513573889145060(-4)	0.1717288384479593…
	-0.7147	-0.9692(-3)	-0.1389(-4)	0.1717(-2)
0.8	-0.30737616937856374699	-0.83285869514776562125(-3)	-0.17724872249838974423(-4)	0.1500441689647712…
	-0.3073	-0.8328(-3)	-0.1772(-4)	0.1500(-2)
0.9	(unbound)			
	0.0307	-0.5512(-3)	-0.1735(-4)	0.1018(-2)

20

References

(1959). *Rev. Mod. Phys.*, *31*, 569.

(1982). *Rev. Mod. Phys.*, *54*, 1017.

(2013). *Phys. Rev. E*, *87*, 063113.

(2015). *Phys. Rev. E*, *91*, 033104.

(1923). *Z. Phys*, *24*, 185.

(1997). *Phys. Rev. A*, *56*, 1642.

(2009). *Adv. Quantum Chem.*, *58*, 115.

(2016). *Matter Radiat. Extremes*, *1*, 237.

(2017). *Phys. Plasmas*, *24*, 122101.

(2020). *Phys. Plasmas*, *27*, 072101.

(2006). *Phys. Rev. B*, *73*, 165210.

(2010). *Phys. Rev. B*, *81*, 125315.

(2008). *Phys. Lett. A*, *372*, 2897.

(2010). *Plasma Phys. Control. Fusion*, *52*, 124040.

(2012). *Phys. Rev. Lett.*, *108*, 165007.

(1960). *J. Phys. Soc. Jan.*, *15*, 928.

(1962). *J. Phys. Chem. Solids*, *23*, 1147.

(1969). *Phys. Rev.*, *178*, 1337.

(1942). *Ark. Mat. Astron. Fys. A*, *28*, 5.

(1990). *Phys. Rev. A*, *41*, 4682.

(2016). *IEEE Trans. Plasma Sci.*, *44*, 2297.

(1971). *Phys. Rev. A*, *4*, 1875.

(1974). *Phys. Rev. A*, *9*, 52.

(1976). *Phys. Rev. A*, *14*, 2363.

(1993). *Phys. Rev. A*, *48*, 220.

(1986). *Phys. Rev. A*, *34*, 5108.

(1987). *Phys. Rev. A*, *35*, 2722.

(1987). *Phys. Rev. A*, *36*, 1045.

(2003). *J. Phys. A: Math. Gen.*, *36*, 11807.

(2007). *Int. J. Quantum Chem.*, *107*, 1040.

(1976). *Phys. Rev. A*, *13*, 532.

(1982). *Phys. Rev. A*, *26*, 2245.

(2005). *Pramana*, *65*, 1.

(2013). *Int. J. Quantum Chem.*, *113*, 1503.

(2016). *Int. J. Quantum Chem.*, *116*, 953.

(2008). *Phys. Rev. A*, *78*, 062511.

(2016). *Phys. Plasmas*, *23*, 073302.

(2009). *Phys. Rev. A*, *80*, 032502.

(2012). *Phys. Plasmas*, *19*, 092707.

(2018). *Chinese J. Phys.*, *56*, 3085.

(2009). *Phys. Rev. A*, *80*, 063404.

(2017). *Phys. Plasmas*, *24*, 062110.

(2018). *Int. J. Quantum Chem.*, *118*, e25620.

(2017). *Mol. Phys.*, *115*, 1480.

(2007). *Chem. Phys.*, *331*, 346.

(2011). *Phys. Scr.*, *84*, 045001.

(2013). *Phys. Plasmas*, *20*, 123301.

(2019). *Phys. Plasmas*, *26*, 033514.

(2014). *Phys. Rev. A*, *90*, 052520.

(2002). *Can. J. Phys.*, *80*, 181.

Quantum Mechanics of One- and Two-Electron Atoms. (2008). Dover Publications, New York.

(2020). *Int. J. Quantum Chem.*, *120*, e26245.

(2004). *Phys. Rev. E*, *69*, 016404.

(2012). *J. Phys. A: Math. Theor.*, *45*, 185302.

(2015). *Phys. Plasmas*, *22*, 012104.

(2017). *Eur. Phys. J. D*, *71*, 71.

(2016). *Rev. Mod. Phys.*, *88*, 035009.

(1993). *Chem. Phys. Lett.*, *204*, 381.

(2004). *Phys. Rep.*, *390*, 1.

Spectral Methods: Fundamentals in Single Domains. (2006). Springer Berlin, Heidelberg.

Numerical Recipes in Fortran 77. (1992). Cambridge University Press, Cambridge.

(2001). *Plasma Phys. Control. Fusion*, *43*, 1119.

(1991). *J. Phys. A: Math. Gen.*, *24*, 2061.

(1978). *J. Math. Phys.*, *19*, 819.

(1992). *Phys. Rev. A*, *46*, 7295.